On Time-Bandwidth Product of Multi-Soliton Pulses

Alexander Span*, Vahid Aref†, Henning Bülow†, and Stephan ten Brink*

*Institute of Telecommunications, University of Stuttgart, Stuttgart, Germany

†Nokia Bell Labs, Stuttgart, Germany

Abstract—**Multi-soliton pulses are potential candidates for fiber optical transmission where the information is modulated and recovered in the so-called nonlinear Fourier domain. While this is an elegant technique to account for the channel nonlinearity, the obtained spectral efficiency, so far, is not competitive with the classic Nyquist-based schemes. In this paper, we study the evolution of the time-bandwidth product of multi-solitons as they propagate along the optical fiber. For second and third order soliton pulses, we numerically optimize the pulse shapes to achieve the smallest time-bandwidth product when the phase of the spectral amplitudes is used for modulation. Moreover, we analytically estimate the pulse-duration and bandwidth of multi-solitons in some practically important cases. Those estimations enable us to approximate the time-bandwidth product for higher order solitons.**

I. Introduction

Advances made over the past decade in coherent optical technology have significantly improved transmission capacities to a point where Kerr nonlinearity once again becomes the limiting factor. The equalization of nonlinear effects is usually very complex and has a limited gain due to the mixing of signal and noise on the channel. The optical channel is usually modeled by the Nonlinear Schrödinger Equation (NLSE) which describes the interplay between Kerr nonlinearity and chromatic dispersion along the fiber.

The Nonlinear Fourier Transform (NFT) is a potential way of generating pulses matched to a channel governed by the NLSE. It maps a pulse to the nonlinear Fourier spectrum with some beneficial properties. This elegant technique, known also as inverse scattering method [1], has found applications in fiber optics when the on-off keying of first order solitons was developed in the 1970s [2]. Following [3], [4], it has regained attention as coherent technology allows to exploit all degrees of freedom offered by the nonlinear spectrum.

Multi-soliton pulses are specific solutions of the NLSE. Using the NFT, an N−th order soliton, denoted here by N−soliton, is mapped to a set of N distinct nonlinear frequencies, called eigenvalues, and the corresponding spectral amplitudes. The key advantage of this representation is that the complex pulse evolution along the fiber can be expressed in terms of spectral amplitudes which evolve linearly in the nonlinear spectrum. Moreover, the transformation is *independent* of the other spectral amplitudes and eigenvalues. These properties motivate to modulate data using spectral amplitudes.

On-off keying of 1-soliton pulses, also called fundamental solitons, has been intensively studied two decades ago for different optical applications (see [2] and reference therein). To increase spectral efficiency, it has been proposed to modulate multi-solitons [3]. One possibility is the independent on-off keying of N predefined eigenvalues. The concept has been experimentally shown up to using 10 eigenvalues in [5], [6]. The other possibility is to modulate the spectral amplitudes of N eigenvalues. The QPSK modulation of spectral amplitudes has been verified experimentally up to 7 eigenvalues in [7], [8], [9]. All of these works have a small spectral efficiency.

Characterizing the spectral efficiency of multi-soliton pulses is still an open problem. First, the statistics of noisy received pulses in the nonlinear spectrum have not yet been fully understood, even though there are insightful studies for some special cases and under some assumptions [10], [11], [12]. Second, the bandwidth and the pulse-duration change as a multi-soliton propagates along a fiber or as spectral amplitudes are modulated. The nonlinear evolution makes it hard to estimate the time-bandwidth product of a multi-soliton.

In this paper, we study the evolution of pulse-duration and bandwidth of multi-soliton pulses along an optical fiber link. We numerically optimize the time-bandwidth product of N−soliton pulses for $N = 2$ and 3. The results provide some guidelines for $N > 3$. We focus on scenarios where the phases of N spectral amplitudes are modulated independently. However, our results can also be applied to on-off keying modulation schemes. We assume that the link is long enough so that the pulse-duration and bandwidth can reach their respective maximum. We also neglect inter-symbol interference. Our results show that the optimization of [13] is suboptimal when the evolution along the fiber is taken into account.

We further introduce a class of N−solitons which are provably symmetric. A subset of these pulses are already used in [7], [8], [13]. We derive an analytic approximation of their pulse-duration. Numerical observations exhibit that the approximation is tight and can serve as a lower-bound for other N−solitons. To the best of our knowledge, this is the first result on the pulse-duration of multi-solitons. We also approximate the time-bandwidth product by lower-bounding the maximal bandwidth.

II. Preliminaries on Multi-Soliton Pulses

In this section, we briefly explain the nonlinear Fourier transform (NFT), the characterization of multi-soliton pulses in the corresponding nonlinear spectrum and how they can be generated via the inverse NFT.

A. Nonlinear Fourier Transform

The pulse propagation along an ideally lossless and noiseless fiber is characterized using the standard Nonlinear Schrödinger Equation (NLSE)

$$\frac{\partial}{\partial z}q(t,z) + j\frac{\partial^2}{\partial t^2}q(t,z) + 2j|q(t,z)|^2 q(t,z) = 0. \quad (1)$$

The physical pulse $Q(\tau, \ell)$ at location ℓ along the fiber is then described by

$$Q(\tau, \ell) = \sqrt{P_0} \; q\left(\frac{\tau}{T_0}, \ell \frac{|\beta_2|}{2T_0^2}\right) \text{ with } P_0 \cdot T_0^2 = \frac{|\beta_2|}{\gamma},$$

where $\beta_2 < 0$ is the chromatic dispersion and γ is the Kerr nonlinearity of the fiber, and T_0 determines the symbol rate. The closed-form solutions of the NLSE (1) can be described in a nonlinear spectrum defined by the following so-called Zakharov-Shabat system [1]

$$\frac{\partial}{\partial t}\begin{pmatrix} \vartheta_1(t;z) \\ \vartheta_2(t;z) \end{pmatrix} = \begin{pmatrix} -j\lambda & q(t,z) \\ -q^*(t,z) & j\lambda \end{pmatrix}\begin{pmatrix} \vartheta_1(t;z) \\ \vartheta_2(t;z) \end{pmatrix}, \quad (2)$$

with the boundary condition

$$\begin{pmatrix} \vartheta_1(t;z) \\ \vartheta_2(t;z) \end{pmatrix} \to \begin{pmatrix} 1 \\ 0 \end{pmatrix} \exp(-j\lambda t) \text{ for } t \to -\infty$$

under the assumption that $q(t;z) \to 0$ decays sufficiently fast as $|t| \to \infty$ (faster than any polynomial). The nonlinear Fourier coefficients (Jost coefficients) are defined as

$$a(\lambda;z) = \lim_{t \to \infty} \vartheta_1(t;z)\exp(j\lambda t)$$
$$b(\lambda;z) = \lim_{t \to \infty} \vartheta_2(t;z)\exp(-j\lambda t).$$

The set Ω denotes the set of simple roots of $a(\lambda;z)$ with positive imaginary part, which are called *eigenvalues* as they do not change in terms of z, i.e. $\lambda_k(z) = \lambda_k$. The nonlinear spectrum is usually described by the following two parts:

(i) Continuous Part: the spectral amplitude $Q_c(\lambda;z) = b(\lambda;z)/a(\lambda;z)$ for real frequencies $\lambda \in \mathbb{R}$.
(ii) Discrete Part: $\{\lambda_k, Q_d(\lambda_k;z)\}$ where $\lambda_k \in \Omega$, i.e. $a(\lambda_k;z) = 0$, and $Q_d(\lambda_k;z) = b(\lambda_k;z)/\frac{\partial a(\lambda;z)}{\partial \lambda}|_{\lambda = \lambda_k}$.

An $N-$soliton pulse is described by the discrete part only and the continuous part is equal to zero (for any z). The discrete part contains N pairs of eigenvalue and the corresponding spectral amplitude, i.e. $\{\lambda_k, Q_d(\lambda_k;z)\}, 1 \le k \le N$.

An important property of the nonlinear spectrum is its simple linear evolution given by [3]

$$Q_d(\lambda_k;z) = Q_d(\lambda_k)\exp(-4j\lambda_k^2 z), \quad (3)$$

where we define $Q_d(\lambda_k) = Q_d(\lambda_k;z=0)$. The transformation is linear and depends only on its own eigenvalue λ_k. This property motivates for modulation of data over independently evolving spectral amplitudes.

Note that there are several methods to compute the nonlinear spectrum by numerically solving the Zakharov-Shabat system. Some of these methods are summarized in [3],[14].

B. Inverse NFT

The Inverse NFT (INFT) maps the given nonlinear spectrum to the corresponding pulse in time-domain. For the special case of the spectrum without the continuous part, the Darboux Transformation can be applied to generate the corresponding multi-soliton pulse [15]. Algorithm 1 shows the pseudo-code of the inverse transform, as described in [16]. It generates an $N-$soliton $q(t)$ recursively by adding a pair $\{\lambda_k, Q_d(\lambda_k)\}$ in

each recursion. The main advantage of this algorithm is that it is exact with a low computational complexity and it can be used to derive some properties of multi-soliton pulses.

Algorithm 1: INFT from Darboux Transform [16]

Input : Discrete Spectrum $\{\lambda_k, Q_d(\lambda_k)\}$; $k = 1, \dots, N$
Output: $N-$soliton waveform $q(t)$

begin
  for $k \leftarrow 1$ **to** N **do**
    $\rho_k^{(0)}(t) \longleftarrow \left(\frac{Q_d(\lambda_k)}{\lambda_k - \lambda_k^*}\prod_{m=1, m \neq k}^{N}\frac{\lambda_k - \lambda_m}{\lambda_k - \lambda_m^*}\right)e^{2j\lambda_k t};$
  $q^{(0)} \longleftarrow 0;$
  for $k \leftarrow 1$ **to** N **do**
    $\rho(t) \longleftarrow \rho_k^{(k-1)}(t);$
    $q^{(k)}(t) \longleftarrow q^{(k-1)}(t) + 2j(\lambda_k - \lambda_k^*)\frac{\rho^*(t)}{1 + |\rho(t)|^2};$

$$\qquad\qquad\qquad\qquad\qquad\qquad\qquad (4)$$

    for $m \leftarrow k+1$ **to** N **do**
      $\rho_m^{(k)}(t) \longleftarrow$
$$\frac{(\lambda_m - \lambda_k)\rho_m^{(k-1)}(t) + \frac{\lambda_k - \lambda_k^*}{1 + |\rho(t)|^2}(\rho_m^{(k-1)}(t) - \rho(t))}{\lambda_m - \lambda_k^* - \frac{\lambda_k - \lambda_k^*}{1 + |\rho(t)|^2}\left(1 + \rho^*(t)\rho_m^{(k-1)}(t)\right)};$$

$$\qquad\qquad\qquad\qquad\qquad\qquad\qquad (5)$$

(λ^* denotes the complex conjugate of λ)

C. Definition of Pulse Duration and Bandwidth

In this paper, we consider an $N-$soliton with the eigenvalues on the imaginary axis, i.e. $\{\lambda_k = j\sigma_k\}_{k=1}^{N}$ and $\sigma_k \in \mathbb{R}^+$. Without loss of generality, we assume that $\sigma_k < \sigma_{k+1}$. As such an $N-$soliton propagates along the fiber, the pulse does not disperse and the pulse shape can be repeated periodically.

An $N-$soliton pulse has unbounded support and exponentially decreasing tails in time and (linear) frequency domain. As this pulse is transformed according to the NLSE, e.g. propagation along the ideal optical fiber, its shape can drastically change as all $Q_d(\lambda_k;z)$ are evolved in z. Despite of nontrivial pulse variation and various peak powers, the energy of the pulse remains fixed and equal to $E_{\text{total}} = 4\sum_{k=1}^{N}\text{Im}\{\lambda_k\}$.

As a result, the pulse-duration and the bandwidth of a multi-soliton pulse are well-defined if they are characterized in terms of energy: the pulse duration T_w (and bandwidth B_w, respectively) is defined as the smallest interval (frequency band) containing $E_{\text{trunc}} = (1-\varepsilon)E_{\text{total}}$ of the soliton energy. Note that truncation causes small perturbations of eigenvalues. In practical applications, the perturbations become even larger due to inter-symbol-interference (ISI) when a train of truncated soliton pulses is used for fiber optical communication. Thus, there is a trade-off: ε must be kept small such that the truncation causes only small perturbations, but large enough to have a relatively small time-bandwidth product.

Note that truncating a signal in time-domain may slightly change its linear Fourier spectrum in practice. For simplicity, we however computed T_w and B_w with respect to the original pulse as the difference is negligible for $\varepsilon \ll 1$.

III. SYMMETRIC MULTI-SOLITON PULSES

In this section, we address the special family of multi-soliton pulses which are symmetric in time domain. An application of such solitons for optical fiber transmission is studied in [7] where the symmetric 2-solitons are used for data modulation.

Theorem 1. *Let* $\Omega = \{j\sigma_1, j\sigma_2, \ldots, j\sigma_N\}$ *be the set of eigenvalues on the imaginary axis where* $\sigma_k \in \mathbb{R}^+$, *for* $1 \leq k \leq N$. *The corresponding* $N-$*soliton* $q(t)$ *is a symmetric pulse, i.e.* $q(t) = q(-t)$, *and keeps this property during the propagation in* z, *if and only if the spectral amplitudes are chosen as*

$$|Q_{d,\mathrm{sym}}(j\sigma_k)| = 2\sigma_k \prod_{m=1; m\neq k}^{N} \left| \frac{\sigma_k + \sigma_m}{\sigma_k - \sigma_m} \right|. \quad (6)$$

Sketch of Proof. The proof is based on Algorithm 1 with the following steps: (i) $g(t) = \frac{\rho^*(t)}{1+|\rho(t)|^2}$ is symmetric, if

$$\rho^*(-t)\rho(t) = 1. \quad (7)$$

(ii) The update rule (5) preserves the property (7): if $\rho(t)$ and $\rho_m^{(k-1)}(t)$ satisfy (7), then $\rho_m^{(k)}(t)$ will satisfy (7) as well.
(iii) Because of (6), $\rho_k^{(0)}(t)$ satisfies (7) for all k.
(iv) Using induction, $\rho_m^{(k)}$ satisfies (7) for all m and k.
(v) According to (4) and step (i), $q(t)$ is symmetric. □

It is already mentioned in [17] that (6) leads to a symmetric multi-soliton in amplitude. Theorem 1 implies that (6) is not only sufficient but also necessary to have $q(t) = q(-t)$.

As it is shown in the next section, we *numerically observe* that these symmetric pulses have the smallest pulse duration[1] among all solitons with the same set of eigenvalues Ω (but different $|Q_d(\lambda_k)|$). Assuming $\sigma_1 = \min_k \{\sigma_k\}$, this minimum pulse-duration can be well approximated by

$$T_{\mathrm{sym}}(\varepsilon) \approx \frac{1}{2\sigma_1} \left(2 \sum_{m=2}^{N} \ln\left(\frac{\sigma_m + \sigma_1}{\sigma_m - \sigma_1} \right) \right.$$
$$\left. + \ln\left(\frac{2}{\varepsilon} \right) - \ln\left(\frac{\sum_{m=1}^{N} \sigma_m}{\sigma_1} \right) \right), \quad (8)$$

where ε is defined earlier as the energy threshold. The approximation becomes tight as $\varepsilon \to 0$ and is only valid if $\varepsilon \ll \sigma_1 / \sum_{m=1}^{N} \sigma_m$. Verification of (8) follows readily by describing an $N-$soliton by the sum of N terms according to (4), and showing that in the limit $|t| \to \infty$, the dominant term behaves as $\mathrm{sech}(2\sigma_1(|t| - t_0))$ for some t_0 and all other terms decay exponentially faster.

IV. TIME-BANDWIDTH PRODUCT

Consider the transmission of an $N-$soliton with eigenvalues $\{j\sigma_k\}_{k=1}^{N}$ over an ideal fiber of length z_L. Each spectral amplitude $Q_d(j\sigma_k; z) = |Q_d(j\sigma_k; z)| \exp(j\phi_k(z))$ is transformed along the fiber according to (3). Equivalently,

$$|Q_d(j\sigma_k; z)| = |Q_d(j\sigma_k; z = 0)|$$
$$\phi_k(z) = \phi_k(0) + 4\sigma_k^2 z$$

[1]It is correct when ε is small enough.

for $z \leq z_L$. It means that $\phi_k(z)$ changes with a distinct speed proportional to σ_k^2. Different phase combinations correspond to different soliton pulse shapes with generally different pulse-duration and bandwidth. It implies that T_w and B_w of a pulse are changing along the transmission. Furthermore, if the $\phi_k(0)$ are independently modulated for each eigenvalue with a constellation of size M, e.g. $M-$PSK, this results in M^N initial phase combinations ($N \log_2(M)$ bits per soliton) associated with different initial pulse shapes. Such transmission scenarios are demonstrated experimentally for $M = 4$, $N = 2$ [7] and $N = 7$ [8]. To avoid a considerable ISI between neighboring pulses in a train of N-solitons for transmission in time or frequency, we should consider T_w and B_w larger than their respective maximum along the link.

For a given set of eigenvalues and fixed $|Q_d(j\sigma_k; z = 0)|$, the maxima depend on M^N initial phase combinations and the fiber length z_L. To avoid these constraints, we maximize T_w and B_w over all possible phase combinations:

$$T_{\max} = \max_{\phi_k, 1 \leq k \leq N} T_w \text{ and } B_{\max} = \max_{\phi_k, 1 \leq k \leq N} B_w.$$

These quantities occur in the worst case but can be reached in their vicinity when N is small, e.g. 2 or 3, or when M is very large, or the transmission length z_L is large enough.

In the rest of this section, we address the following fundamental questions:

(i) How do $T_{\max}$ and $B_{\max}$ change in terms of $\{j\sigma_k\}_{k=1}^{N}$ and $\{|Q_d(j\sigma_k)|\}_{k=1}^{N}$?
(ii) What is the smallest time-bandwidth product for a given N, i.e.

$$(T_{\max} B_{\max})^\star = \min_{\sigma_k, 1 \leq k \leq N} \min_{|Q_d(j\sigma_k)|, 1 \leq k \leq N} T_{\max} B_{\max}$$

and which is the optimal choice for $\{j\sigma_k^\star\}_{k=1}^{N}$ and $\{|Q_d^\star(j\sigma_k^\star)|\}_{k=1}^{N}$.

The following properties preserving the time-bandwidth product decrease the number of parameters to optimize:
(i) If $q(t)$ has eigenvalues $\{j\sigma_k\}_{k=1}^{N}$, then $1/\sigma_1 \cdot q(t/\sigma_1)$ will have eigenvalues $\{j\frac{\sigma_k}{\sigma_1}\}_{k=1}^{N}$ with the same time-bandwidth product. It implies that $T_{\max} B_{\max}$ only depends on the $N-1$ eigenvalue ratios σ_k/σ_1.
(ii) If $\{\phi_k\}_{k=1}^{N}$ corresponds to $q(t)$, then $\{\phi_k - \phi_1\}_{k=1}^{N}$ corresponds to $q(t) \exp(j\phi_1)$. Thus, we assume $\phi_1 = 0$.
(iii) Instead of directly optimizing $\{|Q_d(j\sigma_k)|\}_{k=1}^{N}$, it is equivalent to optimize $\eta_k > 0$ defined by

$$|Q_d(j\sigma_k)| = \eta_k |Q_{d,\mathrm{sym}}(j\sigma_k)|.$$

Using $\{\eta_k\}_{k=1}^{N}$ has two advantages. The first one is the generalization of Theorem 1. If $\{\eta_k\}_{k=1}^{N}$ corresponds to $q(t)$, then $\{1/\eta_k\}_{k=1}^{N}$ corresponds to $q(-t)$. The proof is similar to the one of Theorem 1. Moreover, $\{e^{-2\sigma_k t_0} \eta_k\}_{k=1}^{N}$ corresponds to $q(t+t_0)$. Thus, it suffices to assume $\eta_1 = 1$ and $\eta_2 \in (0, 1]$.

A. Optimization of Spectral Amplitudes

Consider a given set of eigenvalues $\Omega = \{j\sigma_k\}_{k=1}^{N}$. We want to optimize $\{\eta_k\}_{k=2}^{N}$ to minimize $T_{\max} B_{\max}$. Recall that $\{|Q_d(j\sigma_k)|\}_{k=1}^{N}$, and thus $\{\eta_k\}_{k=1}^{N}$ do not change along z.

We present the optimization method for $N = 2$. In this case, there are two parameters to optimize: ϕ_2 and $\eta_2 \in (0, 1]$. Consider a given energy threshold ε. For each chosen η_2, we find $T_{\max}(\varepsilon)$ and $B_{\max}(\varepsilon)$ by exhaustive search. The phase $\phi_2 \in [0, 2\pi)$ is first quantized uniformly by 64 phases. At each phase, a 2-soliton is generated using Algorithm 1 and then $T_w(\varepsilon)$ and $B_w(\varepsilon)$ are computed. To estimate $T_{\max}(\varepsilon)$, another round of search is performed with a finer resolution around the quantized phase with the largest $T_w(\varepsilon)$. Similarly, $B_{\max}(\varepsilon)$ is estimated.

Fig. 1 illustrates $T_{\max}(\varepsilon)$ and $B_{\max}(\varepsilon)$ in terms of $\log(\eta_2)$ for different energy thresholds ε when $\Omega = \{\frac{1}{2}j, 1j\}$. We also depict $B_{\min}(\varepsilon)$, the minimum bandwidth of 2-soliton pulses with a given η_2 and various ϕ_2. Fig. 1 indicates the following features that we observed for any pairs of $\{j\sigma_1, j\sigma_2\}$.

We can see that for any ε, the smallest $T_{\max}$ is attained at $\eta_2 = 1$ ($\log(\eta_2) = 0$) which corresponds to the symmetric 2-soliton defined in Sec. III. We also observe that $B_{\max}$ reaches the largest value at $\eta_2 = 1$ while $B_{\min}$ reaches its minimum.

As $\log(\eta_2)$ decreases, $T_{\max}$ increases gradually up to some point and then it linearly increases in $|\log(\eta_2)|$. The behaviour of $B_{\max}$ is the opposite. It decreases very fast in $|\log(\eta_2)|$ up to some η_2 and then converges slowly to the bandwidth defined by the 1-soliton spectrum with $\lambda = j\sigma_2$. In fact, we have two separate 1-solitons without any interaction when $\eta_2 = 0$. As η_2 increases to 1, the distance between these two 1-solitons decreases, resulting in more nonlinear interaction but smaller $T_{\max}$. The largest $B_{\max} - B_{\min}$ at $\eta_2 = 1$ indicates the largest amount of interaction.

The above features seem general for $N-$solitons. In particular, $T_{\max}$ becomes minimum if the $N-$soliton is symmetric. Moreover, $B_{\max}$ can be lower-bounded by

$$B_{\text{sep}}(\varepsilon) = \frac{2\sigma_N}{\pi^2} \left(\ln\left(\frac{2}{\varepsilon}\right) - \ln\left(\frac{\sum_{k=1}^{N} \sigma_k}{\sigma_N}\right) \right)$$

with $\sigma_N = \max_k \{\sigma_k\}$. The bound becomes tight when an $N-$soliton is the linear superposition of N separate 1-solitons.

We performed such a numerical optimization for $N = 2$ and $N = 3$ and for different $\{\frac{\sigma_k}{\sigma_1}\}_{k=2}^{N}$. For each ε, we found the optimal $\{\eta_k^\star\}_{k=2}^{N}$ with the smallest $T_{\max}(\varepsilon)B_{\max}(\varepsilon)$.

B. Optimization of Eigenvalues

In general, an $N-$soliton has a larger $T_{\max}B_{\max}$ than a 1-soliton but it has also N times, e.g. $Q_d(j\sigma_k)$, more dimensions for encoding data. To have a fair comparison, we use a notion of "time-bandwidth product per eigenvalue" defined as

$$\overline{T \cdot B}_N\left(\{\tfrac{\sigma_k}{\sigma_1}\}_{k=2}^{N}\right) = \frac{1}{N} T_{\max} B_{\max}\left(\{\tfrac{\sigma_k}{\sigma_1}\}_{k=2}^{N}, \{\eta_k^\star\}_{k=2}^{N}\right)$$

where $T_{\max}B_{\max}$ is already optimized in terms of $\{\eta_k\}$, seperately for each eigenvalue combination. This is an important parameter as the spectral efficiency will be $\mathcal{O}(1/\overline{T \cdot B}_N)$. For a 1-soliton with "sech" shape in time and frequency domain, we have

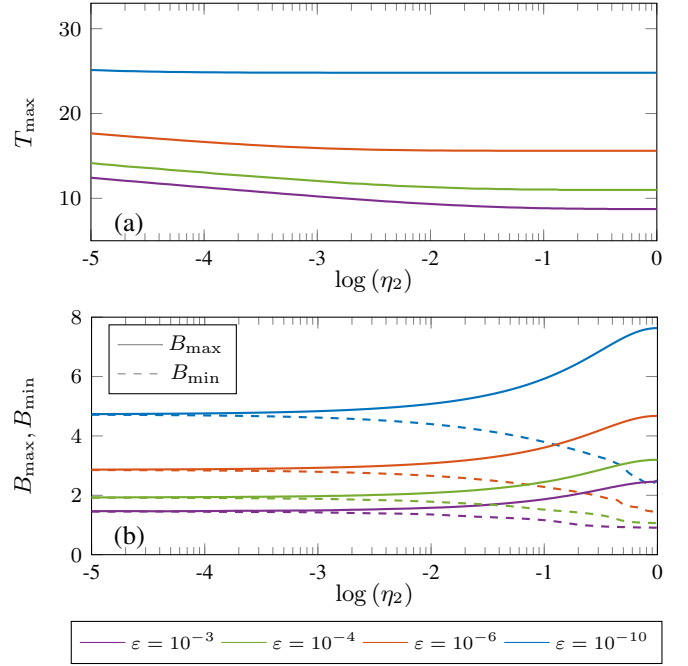$$\overline{T \cdot B}_1 = T_w(\varepsilon)B_w(\varepsilon) = \pi^{-2} \ln^2(2/\varepsilon),$$

Fig. 1. (a) Pulse duration $T_{\max}$ and (b) bandwidth $B_{\max/\min}$ for 2-soliton pulse ($\lambda_1 = 0.5j$, $\lambda_2 = 1j$) when maximized (minimized) over all phase combinations of spectral amplitudes

where ε is the energy threshold defined in Section II-C.

For $N = 2$ and $N = 3$, we numerically optimized $T_{\max}(\varepsilon)B_{\max}(\varepsilon)$ for different values of $\{\frac{\sigma_k}{\sigma_1}\}_{k=2}^{N}$ and $\{\eta_k\}_{k=2}^{N}$. Fig. 2-(a) shows the numerical optimization of $\overline{T \cdot B}_2$ in terms of σ_2/σ_1 for different choices of ε where the best $\{\eta_k^\star\}_{k=2}^{N}$ were chosen for each eigenvalue ratio. We normalized $\overline{T \cdot B}_2$ by $\overline{T \cdot B}_1$ to see how much the "time-bandwidth product per eigenvalue" can be decreased. Fig. 2-(b) shows a similar numerical optimization for $N = 3$ and $\varepsilon = 10^{-4}$. We have the following observations:

(i) $\overline{T \cdot B}_N$ is sensitive to the choice of eigenvalues. For instance, equidistant eigenvalues, i.e. $\sigma_k = k\sigma_1$, are a bad choice in terms of spectral efficiency.

(ii) The ratio $\overline{T \cdot B}_N / \overline{T \cdot B}_1$ gets smaller as ε vanishes. The intuitive reason is that as $\varepsilon \to 0$, we get $T_{\max} \approx \frac{1}{2\sigma_1} \ln(\frac{2}{\varepsilon})$ (see (8)) which is the pulse-duration of the 1-soliton.

(iii) For a practical value of $\varepsilon \sim 10^{-4} - 10^{-3}$, $\overline{T \cdot B}_N$ decreases very slowly in N. Moreover, the optimal $\sigma_k^\star$ are close. This can make the detection challenging in presence of noise. For $\varepsilon = 10^{-4}$,

$$\overline{T \cdot B}_2 / \overline{T \cdot B}_1 = 0.87 \text{ for } \sigma_2^\star/\sigma_1^\star = 1.11$$
$$\overline{T \cdot B}_3 / \overline{T \cdot B}_1 = 0.83 \text{ for } \sigma_2^\star/\sigma_1^\star = 1.28, \sigma_3^\star/\sigma_1^\star = 1.35$$

(iv) Choosing the above optimal $\{\sigma_k^\star/\sigma_1^\star\}$, and the optimal $\{|Q_d^\star(\sigma_k^\star)|\}$, the resulting solitons for $N = 2, 3$ are shown in Fig. 3 for different phase combinations and two energy thresholds ε. This figure gives some guidelines for a larger N: the optimal $N-$soliton has eigenvalues close to each other and significantly seperated pulse centers, why the optimum pulse looks similar to a train of 1-solitons with eigenvalues close to each other. The pulse centers should be close to minimize
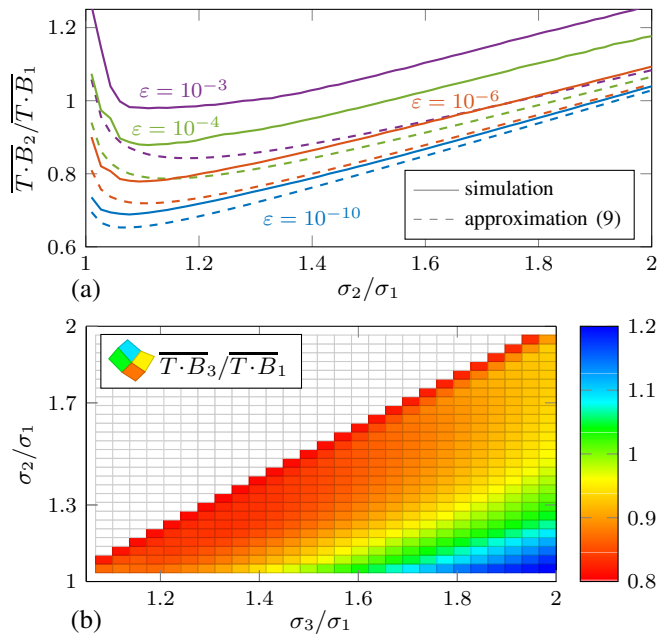
Fig. 2. Gain of time-bandwidth product per eigenvalue of (a) second and (b) third order solitons with eigenvalues $j\sigma_k$ in relation to first order pulses

$T_{\max}$ but not too close to avoid a large interaction which comes along with a growth of $B_{\max}$.
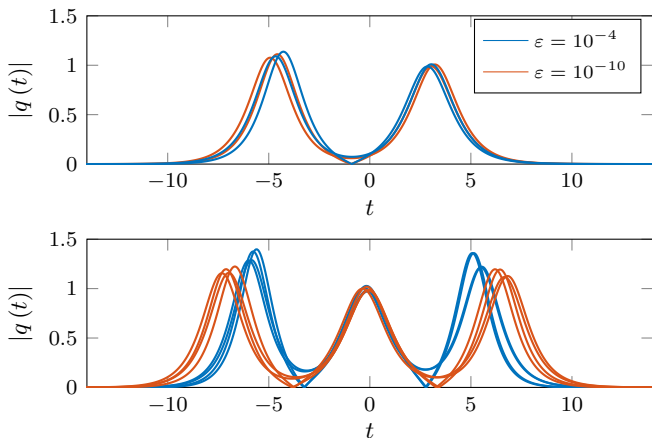

Fig. 3. Time domain signal of optimum second and third order soliton pulse for different phase combinations of the spectral amplitudes (same color)

For $\varepsilon \ll 1$, an estimate on $\overline{T \cdot B}_N$ at optimal $\{\eta_k^*\}$ can be given by (9), where $T_{\max}$ and $B_{\max}$ are estimated by $T_{\text{sym}}(\varepsilon)$ and $B_{\text{sep}}(\varepsilon)$, respectively (see Fig. 1).

$$\overline{T \cdot B}_N \approx \frac{T_{\text{sym}}(\varepsilon) B_{\text{sep}}(\varepsilon)}{N}, \qquad (9)$$

For the second order case, these approximations for various ε are plotted in Fig. 2-(a) by dashed lines. We see that the approximation becomes better for small ε. This approximation can be used to predict $\overline{T \cdot B}_N$ for a large N.

V. CONCLUSION

We studied the evolution of the pulse-duration and the bandwidth of $N-$soliton pulses along the optical fiber. We focused on solitons with eigenvalues located on the imaginary axis. The class of symmetric soliton pulses was introduced and an analytical approximation of their pulse-duration was derived.

The phase of the spectral amplitudes was assumed to be used for modulation while their magnitudes were kept fixed. We numerically optimized the location of eigenvalues and the magnitudes of spectral amplitudes for $2-$ and $3-$solitons in order to minimize the time-bandwidth product. It can be observed that the time-bandwidth product per eigenvalue improves in the soliton order N, but very slowly. Another observation is, that the optimal $N-$soliton pulse looks similar to a train of first-order pulses.

There are some remarks about our optimization. As an $N-$soliton propagates, the phases of the spectral amplitudes change with different speeds. We assumed that all possible combinations of phases occur during transmission. This is the worst case scenario which is likely to happen for $N = 2$ and $N = 3$ but becomes less probable for large N. Moreover, the same magnitudes of spectral amplitudes are used for any phase combination while they can be tuned according to the phases. Without these assumptions, the time-bandwidth product will decrease. However, it becomes harder to estimate as there are many more parameters to optimize.

REFERENCES

[1] A. Shabat and V. Zakharov, "Exact theory of two-dimensional self-focusing and one-dimensional self-modulation of waves in nonlinear media," *Soviet physics JETP*, vol. 34, no. 1, p. 62, 1972.

[2] L. F. Mollenauer and J. P. Gordon, *Solitons in optical fibers: fundamentals and applications*. Academic Press, 2006.

[3] M. Yousefi, F. Kschischang, "Information transmission using the nonlinear fourier transform: I-III," *IEEE Trans. Inf. Theory*, vol. 60, 2014.

[4] J. E. Prilepsky, S. A. Derevyanko, K. J. Blow, I. Gabitov, and S. K. Turitsyn, "Nonlinear inverse synthesis and eigenvalue division multiplexing in optical fiber channels," *Phys. review lett.*, vol. 113, no. 1, 2014.

[5] Z. Dong, S. Hari, *et al.*, "Nonlinear frequency division multiplexed transmissions based on nft," *IEEE Photon. Technol. Lett.*, vol. 27, 2015.

[6] V. Aref, Z. Dong, and H. Buelow, "Design aspects of multi-soliton pulses for optical fiber transmission," in *IEEE Photon. Conf. (IPC)*, 2016.

[7] V. Aref, H. Buelow, K. Schuh, and W. Idler, "Experimental demonstration of nonlinear frequency division multiplexed transmission," in *41st Europ. Conf. on Optical Comm. (ECOC)*, 2015.

[8] H. Buelow, V. Aref, and W. Idler, "Transmission of waveforms determined by 7 eigenvalues with psk-modulated spectral amplitudes," in *42nd Europ. Conf. on Optical Comm. (ECOC)*, 2016.

[9] A. Geisler and C. Schaeffer, "Experimental nonlinear frequency division multiplexed transmission using eigenvalues with symmetric real part," in *42nd Europ. Conf. on Optical Comm. (ECOC)*, 2016.

[10] S. A. Derevyanko, S. K. Turitsyn, and D. A. Yakushev, "Fokker-planck equation approach to the description of soliton statistics in optical fiber transmission systems," *JOSA B*, vol. 22, no. 4, 2005.

[11] Q. Zhang and T. H. Chan, "A spectral domain noise model for optical fibre channels," in *IEEE Int. Symp. on Inf. Theory (ISIT), 2015*, 2015.

[12] S. Wahls, "Second order statistics of the scattering vector defining the d-t nonlinear fourier transform," in *Int. ITG Conf. on Systems, Comm. and Coding (ITG SCC)*, 2017.

[13] S. Hari, M. I. Yousefi, and F. R. Kschischang, "Multieigenvalue communication," *J. Lightw. Technol.*, vol. 34, no. 13, 2016.

[14] S. Wahls and H. V. Poor, "Fast numerical nonlinear fourier transforms," *IEEE Trans. Inf. Theory*, vol. 61, no. 12, 2015.

[15] V. B. Matveev and V. Matveev, *Darboux transformations and solitons*. Springer-Verlag, 1991.

[16] V. Aref, "Control and detection of discrete spectral amplitudes in nonlinear fourier spectrum," *arXiv preprint arXiv:1605.06328*, 2016.

[17] H. A. Haus and M. N. Islam, "Theory of the soliton laser," *IEEE J. Quantum Electron.*, vol. QE-21, no. 8, 1985.